Investigation of target shell effect in heavy ion induced transfer reactions in $^{11}B+^{208}Pb$ and $^{11}B+^{209}Bi$ reactions

P. K. Sahu,[1] A. Saxena,[1] R. K. Choudhury,[1,2] B. K. Nayak,[1] D. C. Biswas,[1] L. M. Pant,[1] R. G. Thomas,[1] and Y. S. Sawant[1]
[1]*Nuclear Physics Division, Bhabha Atomic Research Center, Mumbai 400085, India*
[2]*Institute of Physics, Bhubaneswar 751005, India*
(Received 31 March 2003; published 25 November 2003)

The yields, energy spectra, and angular distributions of the transfer reaction products were measured in $^{11}B+^{208}Pb$ and $^{11}B+^{209}Bi$ reactions at bombarding energies above the Coulomb barrier. It was found that the one-proton pickup cross section is enhanced in $^{11}B+^{209}Bi$ reaction relative to that in $^{11}B+^{208}Pb$ reaction, indicating the influence of target shell closure in the nucleon transfer process. The various aspects of sequential and massive cluster transfers were studied in both reactions from Q value and nucleon mass transfer systematics. The energy spectra and the angular distribution for all the transfer channels were calculated in the framework of diffractional distorted wave Born approximation model for both systems.

DOI: 10.1103/PhysRevC.68.054612 PACS number(s): 25.70.Bc, 24.10.Eq, 25.70.Hi

I. INTRODUCTION

The one- and two-particle transfer reactions have been studied in the past to understand the single-particle shell structure and the pairing correlations in nuclei. The transfer reactions have also been used as a tool to understand the clustering aspects inside the nucleus [1–4]. At below barrier energies, the large enhancements of fusion cross sections are often attributed to the coupling of transfer channels as compared to that expected on the basis of one-dimensional barrier penetration model [5–8]. The measurement of the strength of the one-particle and multiparticle transfer channels and their dependence on shell effects in the target and projectile nuclei are of interest to study the coupling of these channels to the fusion probabilities. The influence of projectile structure in the multinucleon transfer process has been reported in many of the earlier works. However, very little information exists on the study of target shell effects in heavy ion induced transfer reactions. With this motivation we have studied $^{11}B+^{208}Pb$ and $^{11}B+^{209}Bi$ reactions to look for the target shell effects by measuring the one-proton pickup cross sections on the doubly closed shell (^{208}Pb) nucleus and on the target nucleus with one proton outside the closed shell (^{209}Bi). The highly asymmetric systems with a lighter projectile on heavier targets were chosen so that the excitation energy is predominantly in the heavier nucleus having much higher level density, and thus it is unlikely for the lighter projectile to evaporate a particle that would change its identity before it is detected [9]. The relative yields and shapes of the angular distributions of transfer reaction products were measured in both reactions to study the target shell effects. In the past, the distorted wave Born approximation (DWBA) was used to describe the few nucleon transfer processes. However, the DWBA overestimates the absolute cross sections with increase in incident energies [10–13]. For heavy ion reactions occurring well above the Coulomb barrier, continuum states are also strongly populated apart from the first few discrete levels. We have analyzed the transfer reaction data in $^{11}B+^{209}Bi$, ^{208}Pb reactions using a simple model, assuming that the reaction proceeds mainly by one-step processes. There are mainly two ingredients in this model: The first one is the transition matrix element calculated on the basis of diffractional DWBA (DDWBA) model [14,15] and the second ingredient for the calculations is the statistical level density for the population of the continuum states [16–19].

The aim of the present work is to study the effect of target shell closure on transfer cross sections. The data have been analyzed in the framework of DDWBA. The contents of the paper are organized in the following manner. The details of the experimental setup and data analysis along with the ΔN and Q-value systematics and shell effects are discussed in Sec. II. The DDWBA formalism and its application for the calculation of energy spectra and angular distribution of various transfer channels are described in Sec. III. The summary and conclusions of the present work are given in Sec. IV.

II. DETAILS OF EXPERIMENTAL SETUP AND DATA ANALYSIS

The experiments were performed with a ^{11}B beam of 69 MeV bombarding energy accelerated by the 14 UD BARC-TIFR Pelletron accelerator at Mumbai. A self-supporting ^{209}Bi target of 360 $\mu g/cm^2$ thickness and a ^{208}Pb target of 160 $\mu g/cm^2$ thickness on carbon backing of 15 $\mu g/cm^2$ thickness were used in the experiment. Two silicon surface barrier detector telescopes $\Delta E(30\mu m)$-$E(300\mu m)$ and $\Delta E(30\mu m)$-$E(370\mu m)$ were used to measure the angular distributions of the projectilelike fragments. The angular range covered for $^{11}B+^{209}Bi$ and $^{11}B+^{208}Pb$ systems are 45°–80° and 45°–75°, respectively, in steps of 5° in the laboratory frame for both systems. Another silicon surface barrier detector mounted at a fixed angle of $\theta_{lab}=25°$ was used as a beam monitor for relative normalization of different runs. The absolute normalization for the cross section measurements was obtained using elastic scattering data at forward angles and assuming these yields to be described by Rutherford scattering. The ΔE and E detectors in the two telescopes were energy calibrated using the elastic scattering peaks measured at various angles, after taking into account

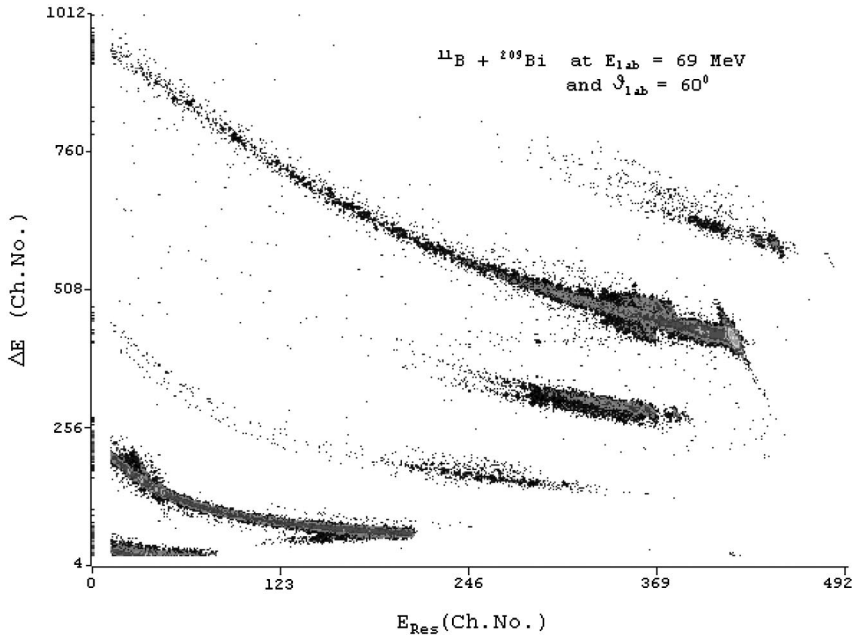

FIG. 1. Typical ΔE vs E_{res} correlation plot for ^{11}B+^{209}Bi reaction at θ_{lab}=60°.

the kinematics and energy loss corrections in the target. A typical two-dimensional ΔE-E_{res} correlation plot for ^{11}B +^{209}Bi reaction at θ_{lab}=60° is shown in Fig. 1, where the masses corresponding to various charges (Z) are seen to be well separated. The transfer channels such as ^{10,12}B can also be clearly identified from the elastic scattering channel as shown in Fig. 1. The mass and charge of the outgoing transfer products were identified using the algorithm, PIO $=\Delta E(E_{res}+a\Delta E+b)\propto MZ^2$, where a and b are constants. The best mass and charge separation between neighboring isotopes was obtained using the values of a=2 and b=15. Typical particle identification spectra obtained in ^{11}B +^{209}Bi and ^{11}B+^{208}Pb reactions around the grazing angle are shown in Fig. 2. Yields of individual isotopes for a given Z were obtained by multiple Gaussian peak fitting to the particle identification spectra. A mass resolution full width at half maximum, of about ≃0.5 amu was achieved in the fitting of the PIO spectra in the present measurements.

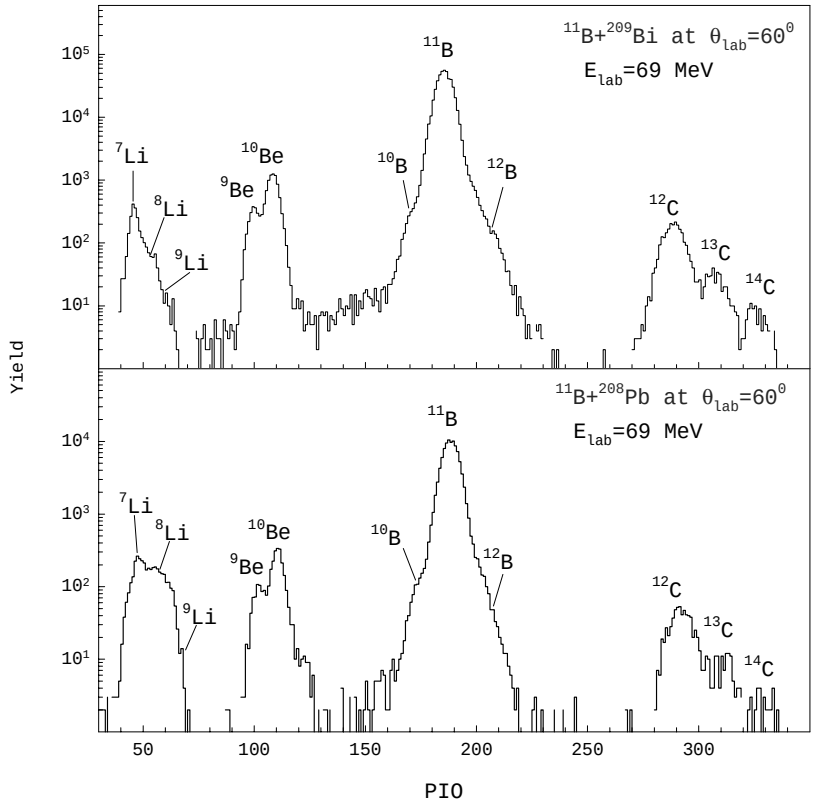

FIG. 2. Typical PIO spectra of ^{11}B+^{209}Bi, ^{208}Pb reactions around their grazing angles.

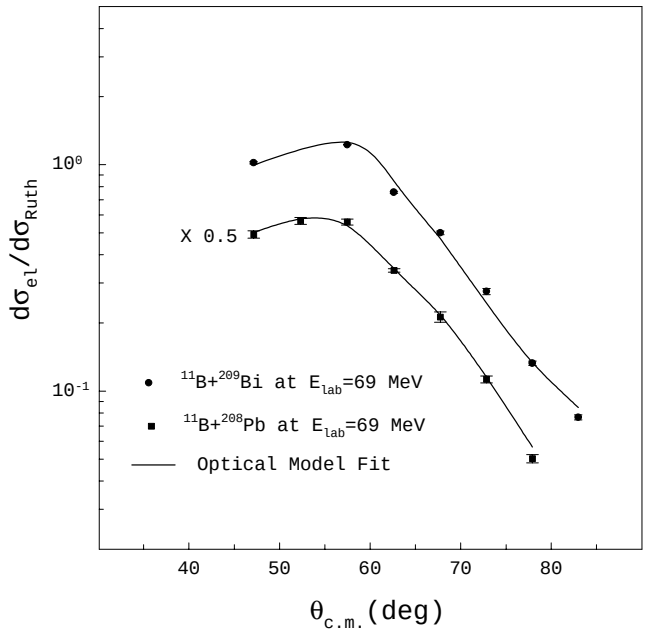

FIG. 3. Ratio of the elastic to Rutherford scattering cross sections as a function of center of mass scattering angles for ^{11}B $+^{209}$Bi, ^{208}Pb systems; the solid lines are fit to the data using optical model code SNOOPY8Q [20].

A. Optical model analysis of elastic scattering cross section

The ratios of elastic to Rutherford scattering cross sections as a function of center of mass scattering angle are shown in Fig. 3 by solid points and solid squares, respectively, for ^{11}B+^{209}Bi and ^{11}B+^{208}Pb systems. These data were analyzed using the optical model code SNOOPY8Q [20] to obtain optical model potential parameters. The results of the fit to the data of $d\sigma_{el}(\theta)/d\sigma_{Ruth}(\theta)$ are shown by solid curves in Fig. 3 for both systems. The potential parameters, the reaction cross sections σ_r, and total cross sections, σ_{total}, obtained from the optical model analysis are listed in Table I. Here, the reaction cross section includes inelastic, transfer, and fusion reaction cross sections, whereas the total cross section also includes elastic scattering cross section. It is seen that in ^{11}B+^{208}Pb reaction all the cross sections are larger than that for ^{11}B+^{209}Bi reaction. This can be accounted by the fact that in the former case the bombarding energy is about 0.5 MeV more above the Coulomb barrier. The fusion cross section σ_f calculated using the CCFUS code [21] is also tabulated in Table I for both systems. The sum of the transfer cross sections integrated over all angles for all the dominant transfer channels (σ_{trans}) are also tabulated in Table I in the last column. It is also seen from the table that the reaction cross section obtained from the optical model analysis by fitting the elastic channels agrees closely with the sum of the transfer and fusion cross sections.

B. *Q* value and ΔN systematics in ^{11}B+^{209}Bi, ^{208}Pb reactions

The experimental angular distributions for the various transfer channels measured in ^{11}B+^{209}Bi and ^{11}B+^{208}Pb reactions are shown by solid points in Figs. 4 and 5, respectively. The angle integrated transfer cross sections σ_{tr} were obtained by integrating the fitted function of angular distribution over the whole solid angle for each of the transfer channels. The angle integrated transfer cross sections as a function of the number of particles transferred (ΔN) for both systems are shown in Fig. 6, where the negative value of ΔN means the particle pickup by the projectile from the target and the positive value of ΔN means the particle stripping from the projectile to the target. The cross section peaks around ΔN=1 stripping channel, and with increasing number of particles picked up or stripped from the projectile, there is near exponential decrease in the cross section, as shown by the dashed lines in Fig. 6. However, deviations are observed in certain transfer channels. It is seen that the cross section for ^{12}B corresponding to one-neutron pickup is enhanced compared to ^{12}C channel corresponding to one-proton pickup. It is also seen that in the stripping reactions ^{7}Li is enhanced and ^{9}Li is suppressed from the systematics of the exponential behavior with the number of nucleons stripped. ^{7}Li channel corresponds to stripping of one α-particle cluster from the projectile, whereas ^{9}Li corresponds to 2p stripping which requires breaking up a proton pair in ^{11}B. These results indicate the importance of the projectile structure and *Q* value effects in the nucleon transfer process. It is known that the transfer cross sections are influenced by the ground state *Q* value for the transfer channels [9]. Figure 7 shows the angle integrated transfer cross section for various transfer channels, σ_{tr} plotted as a function of the ground state reaction *Q* value ($-Q_{gg}$). A nearly bell shaped behavior is observed in both cases as shown by the dashed lines in Fig. 7. Here also certain channels show deviations from the general behavior. There is an optimum value of Q_{gg} of 6–7 MeV, where the cross section is maximum. The enhancement of ^{12}C from the bell shaped *Q*-value systematics is by a factor of 6 and 9 in ^{11}B+^{208}Pb and ^{11}B+^{209}Bi reactions respectively. The ^{7}Li and ^{9}Li also fit into the bell shaped behavior with the *Q* value. The enhancement seen in the 1*p* pickup channel in this plot could be caused by the extra stability of ^{12}C due to N=Z symmetry in this nucleus. However, as discussed in the following section, the relative enhancement of this channel in ^{11}B+^{208}Pb and ^{11}B+^{209}Bi reactions is quite different, which may be connected to double shell closure in the target nucleus after the proton transfer.

TABLE I. Optical model potential parameters and various cross sections.

Systems	V_0 (MeV)	R_0 (fm)	a_0 (fm)	W (MeV)	R_w (fm)	a_w (fm)	r_C (fm)	σ_r (mb)	σ_{total} (mb)	σ_f (mb)	σ_{trans} (mb)
^{11}B+^{209}Bi	19	1.296	0.688	106.99	1.287	0.28	1.3	1143	2173	1043	77.5±1.2
^{11}B+^{208}Pb	19.17	1.241	0.816	100	1.275	0.38	1.3	1302	2347	1077	81.1±1.7

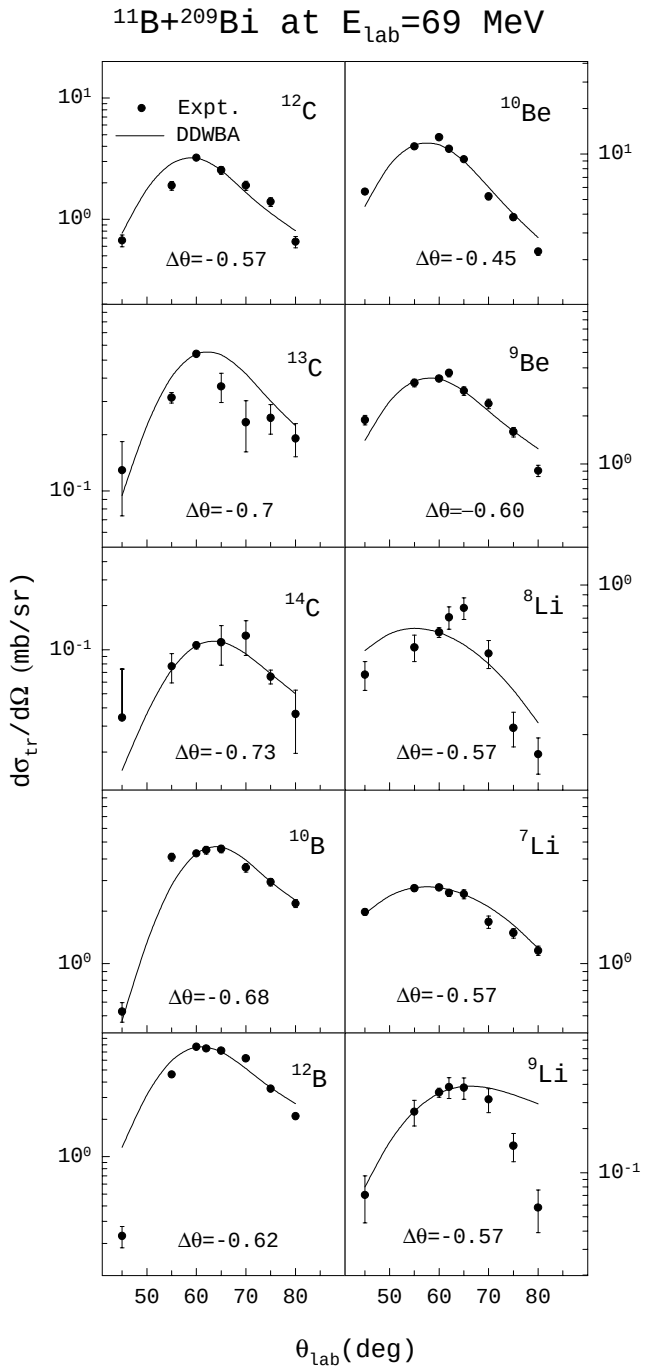

FIG. 4. Angular distribution of various transfer channels in ^{11}B+^{209}Bi reaction with the DDWBA calculation.

C. Shell effects in the heavy ion induced transfer reactions

One of the main motivations of this experiment was to investigate shell effects in the heavy ion induced transfer reactions. We have taken ^{11}B+^{208}Pb and ^{11}B+^{209}Bi systems to compare the one-proton pickup channels in these two reactions. ^{208}Pb is a doubly magic nucleus with closed proton and neutron shells, whereas ^{209}Bi has one extra proton outside the proton shell. Therefore, if one-proton pickup is preferred in ^{11}B+^{209}Bi reaction, as compared to that in ^{11}B +^{208}Pb reaction then it can be inferred that the pickup of the proton is influenced by the shell closure of the target nucleus.

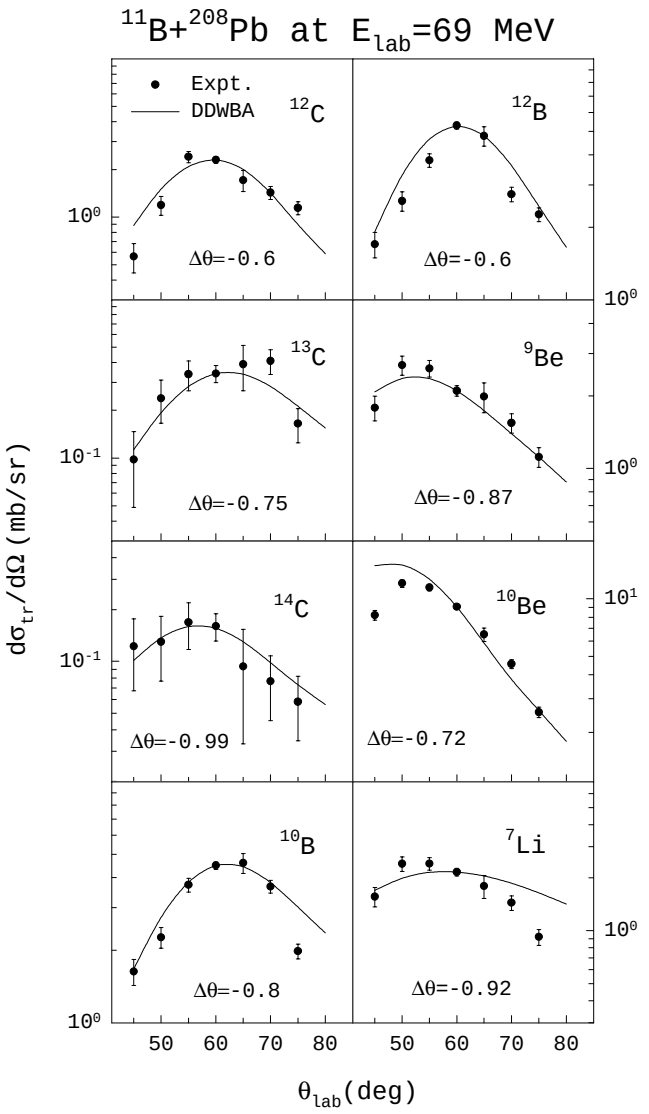

FIG. 5. Angular distribution of various transfer channels in ^{11}B+^{208}Pb reaction with the DDWBA calculations.

In order to study this effect, we examine the ratios of the 1*p* pickup cross section to the 1*n* pickup and stripping cross sections to remove the major nuclear mean field effects that appear in the absolute cross section. The neutron transfer channels in ^{11}B+^{209}Bi, ^{208}Pb transfer reaction will have similar structure effects of the targets due to the closed neutron shell in both ^{209}Bi and ^{208}Pb nuclei. The experimental differential cross section $d\sigma_{expt}/d\Omega$ at the grazing angle, the angle integrated transfer cross section σ_{tr} of ^{12}C, as well as the ratios $\sigma_{tr}(^{12}\mathrm{C})/\sigma_{tr}(^{10}\mathrm{B})$ and $\sigma_{tr}(^{12}\mathrm{C})/\sigma_{tr}(^{12}\mathrm{B})$ for both systems are given in Table II. As can be seen from the table, the experimental differential cross section at the grazing angle, the total, +1*p* cross section, (+1*p*)/(+1n) ratio, and (+1*p*)/(−1n) ratio in ^{11}B+^{209}Bi reaction are all higher as compared to that in ^{11}B+^{208}Pb reaction. The difference is of the order of 42%–86% in the values of the ratios, implying that the transfer of the odd proton in ^{209}Bi is facilitated, so as to drive the target nucleus towards the double shell closure configuration.

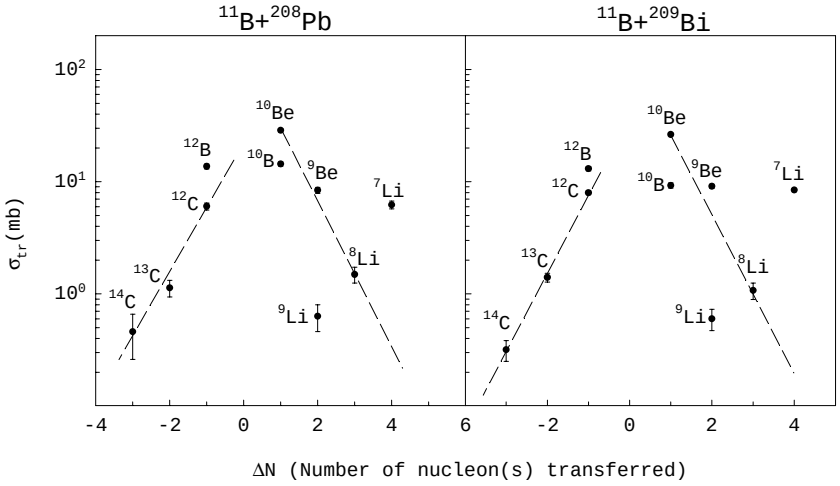

FIG. 6. Total transfer cross section as a function of number of nucleon (s) transferred (ΔN) for ^{11}B+^{209}Bi, ^{208}Pb systems.

III. THEORETICAL UNDERSTANDING OF ENERGY SPECTRA AND ANGULAR DISTRIBUTION OF PROJECTILELIKE FRAGMENTS

The DWBA model has been used to explain the one-particle transfer to discrete states. However, when applied to the continuum states and for multi particle transfers, this model suffers from many limitations. In these cases a modified version called the diffractional DWBA model has been quite successful in explaining the energy spectra and angular distribution of transfer reaction products for a large number of systems [16–19]. In the present work, we have employed the DDWBA model for calculation of one-nucleon and multinucleon transfer cross sections in ^{11}B+^{209}Bi and ^{11}B +^{208}Pb reactions. In this model, the double differential cross section to the continuum states is obtained by weighing the DWBA cross section with the density of states in the projectile and target nuclei, and can be written as [19]

$$\frac{d^2\sigma}{d\Omega dE_f} = \sum_{J_1 J_2} \sum_{L=|J_1-J_2|}^{J_1+J_2} |\tau_L|^2 \int_0^{E_0^*} \rho_1(E_0^* - E_2^*, J_1) \times \rho_2(E_2^*, J_2)\sigma(E_f, \theta, L)dE_2^*. \quad (1)$$

Index 1 is for the ejectile and 2 for the residual nucleus with $E_0^*=E_i+Q_{gg}-E_f$. Here, E_0^* and E_2^* are, respectively, the total and residual nucleus, excitation energies, J_1 and J_2 are the angular momentum of ejectile and residual nucleus, respectively, and $\sigma(E_f, \theta, L)$ is the DWBA cross section, corresponding to a given kinematical condition, with E_i and E_f being the initial and final center of mass kinetic energies. The energy spectrum is calculated by varying E_f from the ground state transition E_i+Q_{gg} up to the exit Coulomb barrier energy. The level density ρ is a function of E_0^* and J [22]. τ_L is called the transfer parameter or the nuclear structure factor, which is an overall normalization constant proportional to the overlaps of the transferred cluster bound state wave functions of the projectile-ejectile and target-residual nuclei multiplied by the product of two corresponding spectroscopic amplitudes. In this formalism, τ_L is assumed to be independent of the energy and the transferred angular momentum for a given transfer reaction. The main ingredient in the DWBA cross section is the reduced matrix element $\beta_{ll'}$, given by

$$\beta_{ll'} = \frac{1}{2i}\sqrt{E_i E_f \frac{\partial \eta_i}{\partial l}\frac{\partial \eta_f}{\partial l'}}\quad e^{i(\sigma_l^i+\delta_l^i+\sigma_{l'}^f+\delta_{l'}^f)}, \quad (2)$$

where σ_l's are the Coulomb phase shifts,

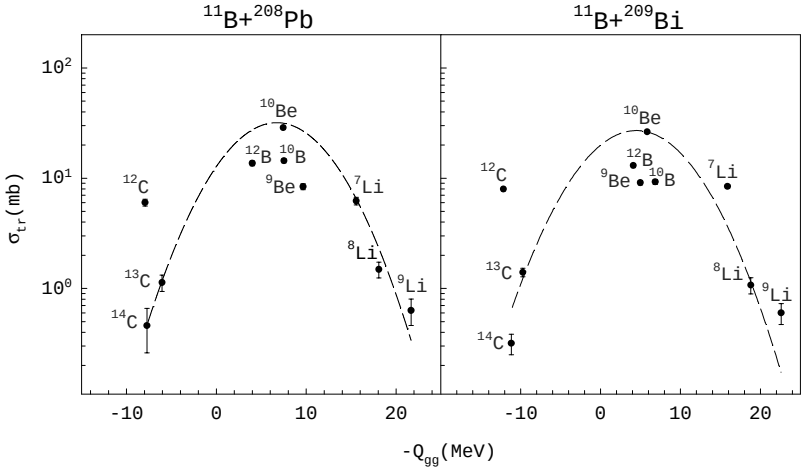

FIG. 7. Total transfer cross section as a function of transfer ground state Q value in ^{11}B +^{209}Bi, ^{208}Pb reactions.

TABLE II. Total transfer cross section ratios of one-nucleon stripping and pickup and various other cross sections of ^{12}C.

Systems	$\left[d\sigma_{expt}/d\Omega\right]_{\theta_{gr}}$ (mb/sr)	$\sigma_{tr}(^{12}C)$ (mb)	$\sigma_{tr}(^{12}C)/\sigma_{tr}(^{10}B)$	$\sigma_{tr}(^{12}C)/\sigma_{tr}(^{12}B)$
^{11}B+^{208}Pb	2.3±0.1	6.0±0.4	0.42±0.04	0.44±0.04
^{11}B+^{209}Bi	3.2±0.03	7.9±0.3	0.86±0.03	0.61±0.04

$$\sigma_l = \arg\,\Gamma(l+1+in), \tag{3}$$

with n being the Sommerfeld parameter in the entrance or the exit channel. δ_l's are the nuclear phase shifts calculated according to the semiclassical parametrization of McIntyre [23]. The reflection coefficient η_l in initial and final channels are parametrized by Woods-Saxon form as [17]

$$\eta_l = \frac{1}{1+\exp\left(\frac{l_g - l}{\Delta}\right)}, \tag{4}$$

where the grazing partial wave l_g and the width Δ are given by the following semi classical relations:

$$l_g = kR\sqrt{1-\frac{2n}{kR}}, \tag{5}$$

$$\Delta = \frac{kd\left(1-\frac{n}{kR}\right)}{\sqrt{1-\frac{2n}{kR}}}. \tag{6}$$

R and d are the radius and the diffuseness parameters, respectively, as determined from the phase-shift analysis of elastic scattering in the entrance and exit channels. In the above formulas the grazing partial wave l_g and width Δ are different in the entrance and exit channels. There is a third parameter in the DWBA cross section, the phase angle $\Delta\theta$, which is the difference between the nuclear and the Coulomb rainbow angles and is related to the nuclear phase-shift. The phase shift analysis of elastic scattering was done by calculating the deflection function given by [24]

$$\Theta(b, E_{\text{c.m.}}) = \pi - 2b\int_{r_{min}}^{\infty} dr\frac{1}{r^2}\left(1-\frac{V_{eff}(b,r)}{E_{\text{c.m.}}}\right)^{-1/2}, \tag{7}$$

where V_{eff} is the total interaction potential between the two colliding nuclei given by

$$V_{eff}(b,r) = V_n(r) + V_C(r) + \frac{b^2 E_{\text{c.m.}}}{r^2}, \tag{8}$$

with b, $E_{\text{c.m.}}$, and r being the impact parameter, center of mass energy, and the distance of separation between the two colliding nuclei, respectively. The real part of the nuclear potential V_n used is of Woods-Saxon shape, obtained by optical model fit to the elastic scattering data. The potential parameters used are taken from Table I. The Coulomb potential V_C is that for two uniformly charged spheres separated by a distance r. The outermost turning point r_{min} is calculated from the equation given below

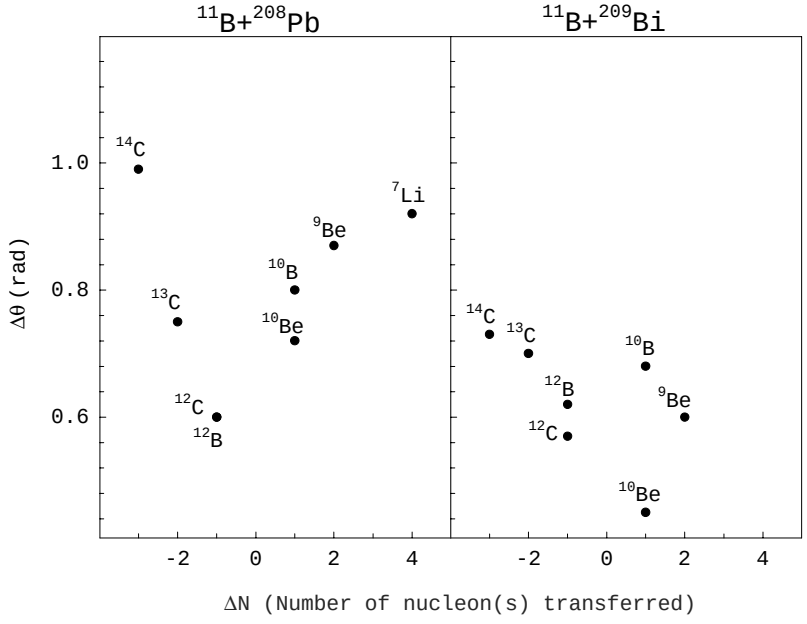

FIG. 8. $\Delta\theta$ as a function of ΔN for ^{11}B +^{208}Pb and ^{11}B+^{209}Bi reactions.

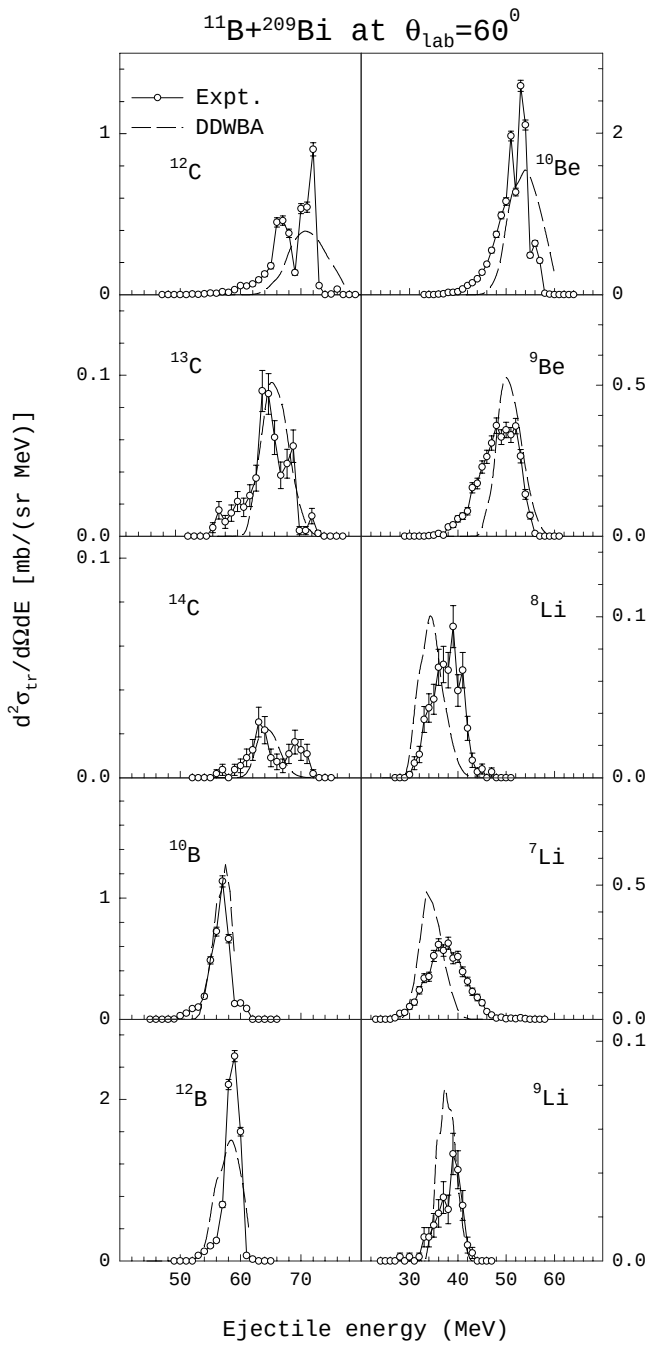

FIG. 9. Energy spectra of various transfer channels in ^{11}B $+^{209}$Bi reaction at the grazing angle with the DDWBA calculation.

$$E_{\mathrm{c.m.}} - V_C(r_{min}) - V_n(r_{min}) - \frac{b^2 E_{\mathrm{c.m.}}}{r_{min}^2} = 0. \qquad (9)$$

From this semiclassical phase-shift analysis, we obtain the grazing l-wave (l_g), the difference between the Coulomb and the nuclear rainbow angle ($\Delta\theta$), and Δ the width at about 75% of the maximum rainbow angles for both systems. The value of l_g and Δ are 30 and 4.54 and 32 and 6.5, respectively, for ^{11}B+^{209}Bi and ^{11}B+^{208}Pb systems. The three parameters r_0, d, and $\Delta\theta$ obtained from the phase-shift analysis are 1.4 fm, 0.59 fm, and –0.57 rad, respectively, for ^{11}B+^{209}Bi system and 1.43 fm, 0.425 fm and −0.78 rad respectively for ^{11}B+^{208}Pb system. However, the value of $\Delta\theta$ had to be adjusted in order to explain the shape of the angular distribution of various transfer channels in both reactions. The value of r_0=1.66 was used to explain the angular distribution of Li channels in ^{11}B $+^{209}$Bi reaction. These parameters were used in the computer code FAST [25] to calculate the angular distributions and the energy spectra at the grazing angles for all the transfer channels in both the reactions. The calculated angular distributions are normalized with the experimental value at the grazing angles for all the transfer channels. The calculated angular distributions of various transfer channels in ^{11}B+^{209}Bi and ^{11}B+^{208}Pb reactions are shown by the solid lines in Figs. 4 and 5, respectively. The corresponding value of $\Delta\theta$ required to fit the angular distribution for each of the transfer channels is also indicated in both figures. The value of $\Delta\theta$ needs to be increased with the increasing number of nucleons transferred to fit the angular distributions in ^{11}B+^{209}Bi, ^{208}Pb reactions, as

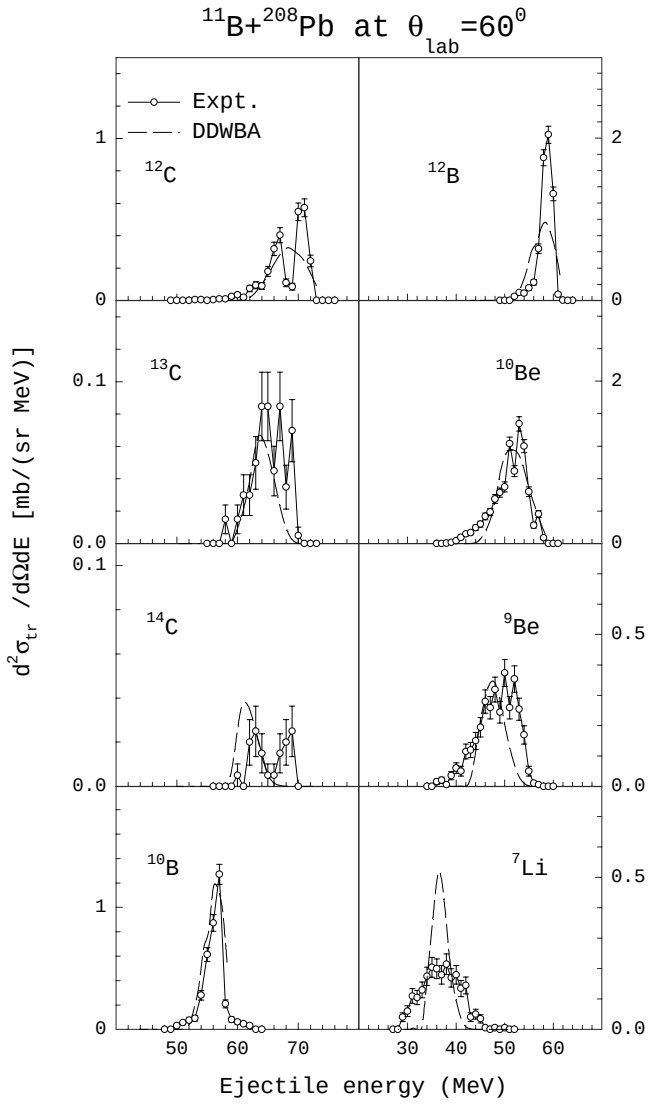

FIG. 10. Energy spectra of various transfer channels in ^{11}B $+^{208}$Pb reaction at the grazing angle with the DDWBA calculation.

shown in Fig. 8. The increase in $\Delta\theta$ is required to shift the angular distribution towards the forward angles. This suggests that the nuclear attraction increases with increasing number of nucleons transferred. The experimental and calculated energy spectra using the DDWBA model are shown in Figs. 9 and 10, respectively, for $^{11}B+^{209}Bi$ and $^{11}B+^{208}Pb$ reactions. As seen from Figs. 4 and 5 and Figs. 9 and 10, the DDWBA model is able to account for the shape of the angular distributions and energy spectra of the reaction products reasonably well. We have kept only the value of $\Delta\theta$ as the free parameter to fit the angular distribution data. The calculated energy spectra generally account for the shift in the peak, but are somewhat narrower than the observed spectra. However, considering the global nature of the fits, the model has succeeded in accounting for the observed features of the transfer reactions in the two systems studied in the present work.

IV. CONCLUSIONS

We have investigated the transfer reactions in $^{11}B+^{209}Bi$ and $^{11}B+^{208}Pb$ systems to study the target shell closure effects in the single-nucleon transfer process. The observed larger values of the one-proton pickup cross section and the ratio of the $1p$ pickup to the $1n$ pickup and $1n$ stripping channels in $^{11}B+^{209}Bi$ reaction as compared to those in $^{11}B+^{208}Pb$ reaction imply the influence of the target shell effect in the heavy ion induced transfer reactions. We have also investigated the various aspects of the multinucleon transfer reactions with regard to the ΔN and Q_{gg} systematics. The diffractional DWBA model was employed to understand the energy spectra and angular distributions of the projectilelike transfer products in both systems. It is seen that this model explains the shape of the angular distribution and energy spectra of the transfer channels to a good extent. A systematic study of the parameters of the DDWBA model has been carried out. The parameter $\Delta\theta$ increases with increasing number of particle transfers, suggesting larger nuclear attraction for higher mass transfers.

ACKNOWLEDGMENTS

The authors acknowledge the help from the accelerator staff of BARC-TIFR pelletron facility, Mumbai, for providing a stable beam during the experiment. We thank R. V. Jangale, V. P. Singh, and A. Inkar for the help rendered during the experiment.

[1] P. K. Sahu, R. K. Choudhury, D. C. Biswas, and B. K. Nayak, Phys. Rev. C **64**, 014609 (2001).
[2] D. C. Biswas, R. K. Choudhury, B. K. Nayak, D. M. Nadkarni, and V. S. Ramamurthy, Phys. Rev. C **56**, 1926 (1997).
[3] L. Corradi, A. M. Stefanini, J. H. He, C. J. Lin, S. Beghini, G. Montagnoli, F. Scarlassara, G. F. Segato, G. Pollarolo, C. H. Dasso, and A. Winther, J. Phys. G **23**, 1485 (1997).
[4] L. Corradi, A. M. Stefanini, C. J. Lin, S. Beghini, G. Montagnoli, F. Scarlassara, G. Pollarolo, and A. Winther, Phys. Rev. C **59**, 261 (1999).
[5] K. E. Rehm, C. Beck, A. Van den Berg, D. G. Kovar, L. L. Lee, W. C. Ma, F. Videbaek, and T. F. Wang, Phys. Rev. C **42**, 2497 (1990).
[6] S. Steadman and M. J. Rhoades-Brown, Annu. Rev. Nucl. Sci. **36**, 649 (1986).
[7] M. Beckerman, Rep. Prog. Phys. **51**, 1047 (1988).
[8] K. E. Rehm, F . L. H. Wolfs, and W. Henning, Phys. Rev. Lett. **55**, 280 (1985).
[9] J. S. Karp, S. G. Steadman, S. B. Gazes, R. Ledoux, and F. Videbaek, Phys. Rev. C **25**, 1838 (1982).
[10] C. Olmer, M. C. Mermaz, M. Buenerd, C. K. Gelbke, D. L. Hendrie, J. Mahoney, D. K. Scott, M. H. Macfarlane, and S. C. Pieper, Phys. Rev. C **18**, 205 (1978).
[11] T. Tamura, T. Udagawa, and M. C. Mermaz, Phys. Rep. **65**, 346 (1980).
[12] T. Udagawa, T. Tamura, and B. T. Kim, Phys. Lett. **82B**, 349 (1979).
[13] T. Udagawa and T. Tamura, Phys. Rev. Lett. **41**, 1770 (1978).
[14] N. Austern and J. S. Blair, Ann. Phys. (N.Y.) **33**, 15 (1965).
[15] F. J. W. Hahne, Nucl. Phys. **A104**, 545 (1967).
[16] M. C. Mermaz, Phys. Rev. C **36**, 1000 (1987).
[17] M. C. Mermaz, Phys. Rev. C **20**, 1962 (1979).
[18] M. C. Mermaz, Phys. Rev. C **21**, 2356 (1980).
[19] M. C. Mermaz, F. Auger, and B. Fernandez, Phys. Rev. C **28**, 1587 (1983).
[20] P. Schwandt, computer code SNOOPY8Q (Indiana University, Indiana, 1984).
[21] J. Fernandez-Niello, C. H. Dasso, and S. Landowne, Comput. Phys. Commun. **54**, 409 (1989).
[22] F. C. Williams, Jr., Nucl. Phys. **A166**, 231 (1971).
[23] A. Pagano, S. Aiello, E. De Filippo, G. Lanzano, S. Lo Nigro, C. Milone, G. Blancato, G. Di Marco, and M. C. Mermaz, Phys. Rev. C **47**, 1170 (1993).
[24] B. K. Nayak, R. K. Choudhury, D. C. Biswas, L. M. Pant, A. Saxena, D. M. Nadkarni, and S. S. Kapoor, Phys. Rev. C **55**, 2951 (1997).
[25] M. C. Mermaz, Saclay Internal report, 1979.